RADIATION RESEARCH **169**, 28–37 (2008)
0033-7587/08 $15.00

Increased Levels of Numerical Chromosome Aberrations after *In Vitro* Exposure of Human Peripheral Blood Lymphocytes to Radiofrequency Electromagnetic Fields for 72 Hours

Ronit Mazor,[a,1] Avital Korenstein-Ilan,[a,1] Alexander Barbul,[a] Yael Eshet,[b] Avi Shahadi,[b] Eli Jerby[b] and Rafi Korenstein[a,2]

[a] *Department of Physiology and Pharmacology, Sackler School of Medicine, and* [b] *Department of Physical Electronics, School of Electrical Engineering, Faculty of Engineering, Tel Aviv University, Israel*

Mazor, R., Korenstein-Ilan, A., Barbul, A., Eshet, Y., Shahadi, A., Jerby, E. and Korenstein, R. Increased Levels of Numerical Chromosome Aberrations after *In Vitro* Exposure of Human Peripheral Blood Lymphocytes to Radiofrequency Electromagnetic Fields for 72 Hours. *Radiat. Res.* 169, 28–37 (2008).

We investigated the effects of 72 h *in vitro* exposure of 10 human lymphocyte samples to radiofrequency electromagnetic fields (800 MHz, continuous wave) on genomic instability. The lymphyocytes were exposed in a specially designed waveguide resonator at specific absorption rates (SARs) of 2.9 and 4.1 W/kg in a temperature range of 36–37°C. The induced aneuploidy of chromosomes 1, 10, 11 and 17 was determined by interphase FISH using semi-automated image analysis. We observed increased levels of aneuploidy depending on the chromosome studied as well as on the level of exposure. In chromosomes 1 and 10, there was increased aneuploidy at the higher SAR, while for chromosomes 11 and 17, the increases were observed only for the lower SAR. Multisomy (chromosomal gains) appeared to be the primary contributor to the increased aneuploidy. The effect of temperature on the level of aneuploidy was examined over the range of 33.5–40°C for 72 h with no statistically significant difference in the level of aneuploidy compared to 37°C. These findings suggest the possible existence of an athermal effect of RF radiation that causes increased levels of aneuploidy. These results contribute to the assessment of potential health risks after continuous chronic exposure to RF radiation at SARs close to the current levels set by ICNIRP guidelines.

INTRODUCTION

The rapid growth in the use of cellular phones with the consequent exposure of large human populations to radiofrequency (RF) electromagnetic fields (EMFs) has led in recent years to a number of studies of the health effects of radiations used in mobile communication. Concerns have been raised regarding the potential of RF EMFs to initiate and/or promote solid and hematological malignancies by inducing genetic alterations and chromosomal aberrations. Most findings so far [for reviews see refs. (*1, 2*)] suggest that exposure of mammalian cells and animals to RF radiation does not cause direct genotoxic effects as assessed from the extent of DNA strand breaks and the incidence of chromosomal aberrations, micronuclei and sister chromatid exchanges. However, the studies are hard to compare because of the different experimental parameters employed, including the cell or animal model, the specific absorption rate (SAR), the duration of chronic continuous or intermittent exposure, and the genetic and/or epigenetic end points examined. It should be stressed that the appropriate selection of an assay(s) to assess the risk for cancer induction by RF EMFs should take into account its nonionizing character.

The etiology of cancer is not fully understood. However, it is known that both genetic (*3–6*) and epigenetic mechanisms are involved (*7–9*). To date, numerical chromosome aberrations, or aneuploidy, the loss and gain of chromosomes, are considered a hallmark of human cancer and are frequently noted in malignant tumors and preneoplastic conditions (*3, 6, 10*). Evidence such as tumor-specific aneuploidy and the presence of mutations in mitotic checkpoint genes suggests that aneuploidy may play an active role in the pathogenesis of cancer (*11*). However, there is much controversy about its cause and effect in relation to malignant tumors (*3, 7, 12–14*). Cancer is considered to be a multistep process, and there is a large body of experimental evidence that variation in nuclear DNA content and chromosomal aneuploidies may occur at early stages of tumorigenesis (*15*). According to this view, gaining or losing entire chromosomes could be considered as the first stage of carcinogenesis. At the second stage, the aneuploid cell generates new karyotypes autocatalytically (*5, 11*). In light of the association between aneuploidy and cancer, it appears that aneuploidy, as a marker of genomic instability (*10, 16–20*), can serve as a valuable genetic marker for cancer risk assessment.

In a previous study we demonstrated an SAR-dependent increase in the aneuploidy of chromosome 17 in human peripheral blood lymphocytes (PBLs) using interphase FISH

[1] R Mazor and A. Korenstein-Ilan contributed equally to this work.

[2] Address for correspondence: Department of Physiology and Pharmacology, Sackler School of Medicine, Ramat Aviv, 69978, Israel; e-mail: korens@post.tau.ac.il.

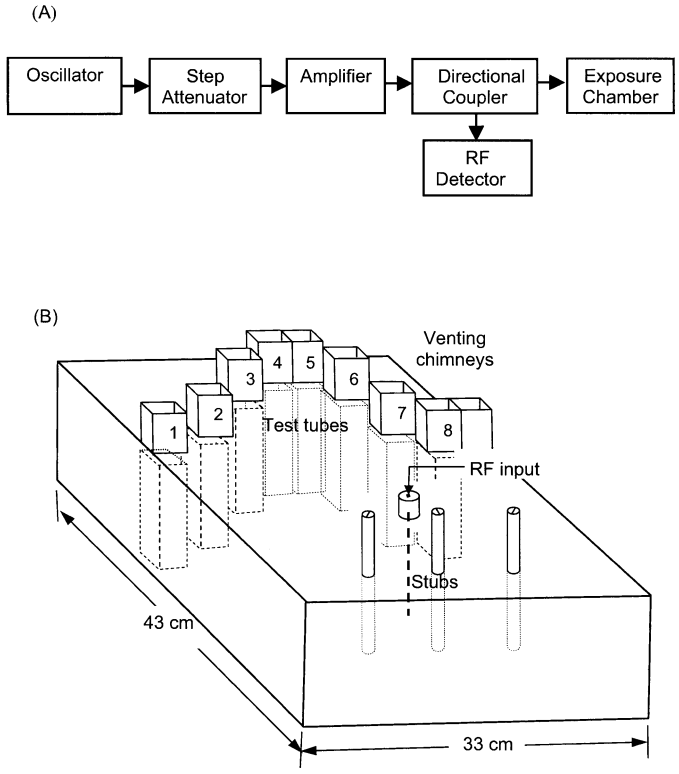

FIG. 1. Exposure setup. Panel A: Block diagram; panel B: schematic representation of the waveguide resonator. The venting chimneys show the placement of the culture tubes in the waveguide. Three perturbation stubs, located between the RF-field input and the waveguide wall, enabling fine tuning of the frequency of the maximal absorption.

(*21*). However, in that study, the cells were exposed to a heterogeneous SAR distribution in the parallel resonator. To expose the cells to a more homogeneous SAR, we constructed an exposure system based on a waveguide resonator. In the present study, we examined changes in the aneuploidy of chromosomes 1, 10, 11 and 17 in human PBLs after *in vitro* exposure in a waveguide resonator to an 800 MHz continuous-wave (CW) electromagnetic field for 72 h.

MATERIALS AND METHODS

Cultures

Human PBLs (5 ml) were obtained from 14 healthy male donors 23 to 39 years old (average 29.7 ± 4.9) in accordance with the Tel-Aviv University Institutional Review Board (Helsinki committee) using a syringe washed with heparin. An aliquot of 0.6 ml of blood was introduced into each of six polystyrene round-bottom test tubes (catalog no. 142AS; Sterilin, UK) containing 4.4 ml of RPMI-1640 medium supplemented with 20% FCS, 1% antibiotics (10,000 U/ml penicillin, 10 mg/ml streptomycin and 1250 U/ml nystatin), 3% PHA-M (all from Biological Industries, Israel), and 0.2% heparin (5000 U/ml, Evans-Promedico, Israel).

Exposure System Design and Verification

The exposure setup shown schematically in Fig. 1A consists of the exposure chamber illustrated in Fig. 1B fed by a controlled microwave generator. The latter includes a tunable oscillator in a cascade with a step attenuator (1-dB steps up to 7 dB) and an RF-signal amplifier. A directional coupler and power detectors enable measurements of the incident power in the exposure chamber and of the power reflected back (i.e. a reflecto-meter setup). The maximum input power available from the generator is 3 W (~34.8 dBm), which can be reduced by the step attenuator to provide the required SAR. The oscillator frequency is tunable in the range between 796 and 892 MHz at 4 MHz intervals. In these experiments, the frequency was set to 0.8 GHz, and the generator output power was 2.4 W. The measured reflected power from the exposure system was 0.6 W; therefore, the absorbed power in the exposure system was 1.8 W (~32.6 dBm).

The custom-made exposure chamber illustrated in Fig. 1B was designed to accommodate eight test tubes with cultures, each exposed at a different SAR. This arrangement enables a wide range of exposure of cultures obtained from the same blood donation simultaneously, thus improving the controllability and validity of the measurements. The variable stubs (Fig. 1B) enable the fine tuning of the exposure. In addition, the closed waveguide structure prevents electromagnetic leakage from the exposure setup, as is the case for parallel-plate devices (*21*). The electromagnetic-wave propagation in the exposure chamber (Fig. 1B) loaded with the test tubes was simulated by 3D numerical electromagnetic-field simulation software (Ansoft HFSS, High Frequency Simulation Software, Version 10.0). The SAR distribution in the exposure chamber and in each test tube was calculated after measuring the specific dielectric properties of the cultures used in the study. Simulations of two types were performed: local SAR and average SAR. The purposes of the local SAR simulations are to account for hot spots and to evaluate the maximal SAR levels throughout the test-tube medium with high precision. Therefore, the simulation adaptive Finite-Element Grid was limited to pixels with a maximum volume of less than 1 mm^3. The average SAR simulations used standard 1-g averaging (for the specific medium). In both the local and average SAR simulations, vertical and horizontal SAR cross sections of the test tubes were calculated. Local SAR simulations were used for exact calculations and averaged ones for the visualization of the spatial distribution.

The temperature in each test tube was measured using a fiber-optic thermometer (Fiso Technologies Inc., Canada) with negligible interference from the electromagnetic radiation. The fiber-optic gage incorporates an 0.8-mm-diameter and 7-mm-long Fabry-Perot cavity located 3 mm from the sensor tip. These fiber-optic sensors, which were introduced vertically through tube's cap all the way to the tube's bottom, were used to monitor steady-state temperature in the test tubes. These sensors were also used in calculating SAR levels from the initial slope of the temperature increase immediately after the RF-field exposure was started. Taking into account the physical dimensions of the temperature sensor and the fact that the cells are located at the very base of the test tube, an accurate assessment of the SARs at the cells' locations was possible only by numerical simulation. Validation of the simulation model for the experimental setup was performed by comparing the numerical simulation with the results derived from the initial slope of the temperature increase assessed by the fiber-optic thermometry. Calculations were performed at tube 4's cross sections equally spaced along the sensing zone of the thermo-optic probes. Comparison of the measured and simulated SARs is presented in the Results section.

Experimental Design

Using PBLs from 10 volunteers, we set up 10 independent exposure experiments in which we used slots 4 and 6 only (SARs of 2.9 and 4.1 W/kg). For each experiment, six culture test tubes were set up: two exposed, two controls and two shams. The test tubes were centrifuged at 100*g* for 7 min to let all cells sink to the bottom of the tubes without being too packed. Thus all the cells in each test tube were exposed to an SAR of high homogeneity at 800 MHz for 72 h. Once every 24 h the exposure system was turned off briefly, and all cultures (exposed, controls and sham) were taken out of the respective incubators, gently mixed and then centrifuged as described and returned to their respective positions in the waveguide resonator, which was placed in an incubator with a humid atmosphere of 95% air/5% CO_2 at 33.5°C (exposed), to the shelf under the waveguide resonator (sham), or to the control incubator (control). The temperature of the exposure incubator was chosen so that dur-

ing exposure the culture temperature would reach about 36.5–37.5°C due to the heating that occurs during irradiation. Test tubes with cells, each marked to identify the exposure condition, were inserted into slots 4 and 6 of the resonator. Two test tubes marked as ''sham exposed'' were placed in a holder on a bottom shelf of the same incubator. We inserted dummy test tubes filled with 5 ml of medium into the other slots of the exposure system to preserve constant electric-field distribution in the resonator. Two test tubes marked as ''control'' were placed in another incubator set at 37°C in a humid atmosphere of 95% air/5% CO_2.

Temperature Dependence of Aneuploidy

Cultures from four different donors were incubated for 72 h in incubators set at four different temperatures: 33.5, 37, 38.5 and 40°C. The temperature in each incubator was maintained with an accuracy of ±0.5°C that was confirmed twice a day using two calibrated thermometers.

Harvest

At 72 h after the cultures were set up, the cells were transferred to 15-ml conical polypropylene test tubes (Corning, catalog no. 430052) and harvested according to standard cytogenetic protocols (*22*). Briefly, colchicine (Biological Industries) was added to a final concentration of 5×10^{-7} *M* for 1 h followed by hypotonic treatment (0.06 *M* KCl at 37°C for 12 min) and four washes with a fresh cold (−20°C) 3:1 methanol:acetic acid solution. Nuclear suspensions were stored at −80°C until used for analysis.

Fluorescence In Situ Hybridization

We performed two-color FISH by combining probes recognizing the centromeres of chromosomes 1 and 10 (Vysis Inc., catalog nos. 32-180001 and 32-132010, respectively) and the probes recognizing the centromeres of chromosomes 11 and 17 (Vysis Inc., catalog nos. 32-130011 and 32-132017, respectively). We essentially followed a standard protocol recommended by Insitus Biotechnologies. The probes were diluted 700-fold using DenHyb D001 (Insitus Biotechnologies). Then 5 μl of the probe solution was placed on the marked spot on the slide and covered with 12-mm round silianized cover slips (Insitus Biotechnologies). Co-denaturation of nuclei and probe was performed in a slide moat (model 240000; Boekel Scientific) at 90°C for 6 min, and slides were then transferred to a covered humidified aluminum tray and placed in a 37°C incubator overnight. Slides were postwashed at 78°C for 4 min in each of the following postwashing solutions: 0.4× SSC (1× SSC = 150 m*M* NaCl, 15 m*M* sodium citrate) with 0.3% NP40 and the second 2× SSC with 0.1% NP40. After excess liquid was removed, slides were treated with 15 μl of an antifade solution containing 3 μg/ml of 4,6-diamino-2-phenylindole (DAPI) as counterstain (Vectashield, Vector Labs), covered with glass cover slips, and stored in the dark at −20°C until microscope analysis.

Analysis

Manual correction was performed on the automated galleries acquired using the Metacyte system (MetaSystems, Altlussheim, Germany), which is a fluorescence object-finding and relocation system. It is based on a fully motorized Axioplan2 microscope (Zeiss), a motorized eight-slide scanning stage (Marzhauser), a high-resolution CCD camera with on chip integration, and a PC equipped with appropriate modules for accurate stage movement and fast image analysis. Metafer 4 is an image analysis software program designed to automatically perform spot counting based on an algorithm (classifier) prepared and optimized by the user. This algorithm takes into account the shape and size of the nuclei as well as the shape, size and relative intensity of the spots counted. To help avoid scoring cells that were not affected by the mitogenic stimulus of PHA, we restricted our analysis to nuclei with an area greater than 50 μm^2. We also excluded from analysis any nuclei that were nullisomic for either of the two chromosomes studied. It should be noted that one of the shortcomings of an automated analysis is the inclusion of all the scanned fields without the subjective skipping performed by a trained observer of areas that are less than optimal, which are always present in a cytogenetic preparation.

The level of aneuploidy was determined in 1237 ± 293 interphase nuclei that were scored for the number of signals representing the number of chromosomes in those cells. The incidence of aneuploidy is calculated as the proportion of nuclei with less than the expected two signals (monosomy) or more than the expected two signals (multisomy) and is given in Table 1 for each individual for each treatment for each chromosome. Table 2 lists the incidence of multisomy for each individual for each treatment for each chromosome. For chromosomes 11 and 17 we performed 10 independent experiments, and for chromosomes 1 and 10 we performed five independent experiments.

Metaphase Index

To estimate the proliferation rate of the samples at the different temperatures, the metaphase index was calculated. The same slides that were scanned and analyzed for aneuploidy were used to determine the proportions of metaphase cells out of about 1000 nuclei by manual scoring.

Statistical Analysis

Changes in chromosome number were calculated as the ratio of the levels in the exposed and the control samples. Statistical significance was tested using the one-sample *t* test (SPSS). *P* values of 0.05 or less were considered statistically significant.

RESULTS

Dosimetry

All the simulated SARs are presented for an incident power level of 1.8 W, as measured for the exposure system setup (Fig. 1). Figure 2 shows the average SAR levels in the eight-tube array, presented at the resonator's transverse cross section (Fig. 2A) and at a median horizontal cross section through the circumference of the tubes (Fig. 2B). The SAR profiles for both the local and average simulations display the highest levels at the middle of the medium in each tube. Such an SAR distribution is caused by the exposure system's transverse field pattern and resulting field boundary conditions at the test tube's facets (i.e., tangential and perpendicular boundary conditions for the electric fields at the longitudinal and bottom facets of the test tubes, respectively). For the local SAR simulation, the maximal SARs in the medium at the center of the tubes range from 0.25 ± 0.06 W/kg in test tube 1 to 11.7 ± 1.0 W/kg in test tube 6, whereas the SARs decrease in the test tubes close to the resonator walls (Fig. 2A and B).

The SAR in each test tube was also assessed by measuring the slope of the initial temperature increase in the medium in each test tube using fiber-optic-based thermometry. The comparison of the measured and numerically calculated SARs is shown in Fig. 3. Numerical calculations were performed by averaging four local SARs taken equidistant across the thermo-sensor location (3–10 mm from the tube base along the longitudinal axis). The calculated SARs at the optical probe locations ranged from a minimum of 0.91 ± 0.14 W/kg (tube 1) to a maximum of 5.13 ± 0.48 W/kg (tube 6), and measured SARs varied from 0.83 ± 0.09 to 7.40 ± 1.76 W/kg in tubes 1 and 6, re-

TABLE 1
Incidence of Aneuploidy for Chromosomes 1, 10, 11 or 17 in Nuclei of Human Blood Lymphocytes Exposed *In Vitro* for 72 h to 800 MHz Radiation at SARs of 2.9 W/kg and 4.1 W/kg for each Individual Tested

	Control			2.9 W/kg			4.1 W/kg		
Donor no.	No. scored	No. aneuploid	Percentage aneuploid	No. scored	No. aneuploid	Percentage aneuploid	No. scored	No. aneuploid	Percentage aneuploid
Chromosome 17									
1	1183	151	12.76	993	170	17.12	794	143	18.01
2	1100	220	20.00	848	121	14.27	1202	215	17.89
3	956	184	19.25	1000	216	21.60	1024	161	15.72
4	1365	208	15.24	1188	161	13.55	1138	173	15.20
5	1449	264	18.22	1006	247	24.55	1047	208	19.87
6	1262	192	15.21	722	146	20.22	1173	217	18.50
7	927	141	15.21	1330	224	16.84	1451	267	18.40
8	1762	359	20.37	1416	362	25.56	1418	280	19.75
9	992	221	22.28	1514	378	24.97	1346	371	27.56
10	1375	291	21.16	1185	323	27.26	1485	441	29.70
Chromosome 11									
1	1183	117	9.89	993	121	12.19	794	81	10.20
2	1100	150	13.64	848	87	10.26	1202	152	12.65
3	956	130	13.60	1000	152	15.20	1024	112	10.94
4	1365	161	11.79	1188	113	9.51	1138	115	10.11
5	1449	162	11.18	1006	152	15.11	1047	144	13.75
6	1262	116	9.19	722	85	11.77	1173	117	9.97
7	927	105	11.33	1330	181	13.61	1451	198	13.65
8	1762	226	12.83	1416	245	17.30	1418	195	13.75
9	992	131	13.21	1514	238	15.72	1346	236	17.53
10	1375	222	16.15	1185	254	21.43	1485	286	19.26
Chromosome 1									
6	953	146	15.32	1706	265	15.53	1641	263	16.03
7	1423	189	13.28	1218	178	14.61	1988	336	16.90
8	1555	273	17.56	674	142	21.07	1196	243	20.32
9	686	103	15.01	1234	282	22.85	1196	292	24.41
10	1471	229	15.57	1546	269	17.40	1543	280	18.15
Chromosome 10									
6	953	131	13.75	1706	209	12.25	1641	219	13.35
7	1423	192	13.49	1218	176	14.45	1988	386	19.42
8	1555	250	16.08	674	161	23.89	1196	249	20.82
9	686	103	15.01	1234	244	19.77	1196	223	18.65
10	1471	201	13.66	1546	250	16.17	1543	233	15.10

spectively. The agreement between the results obtained using these two approaches fit well for the low SARs (slots 1–3 and 8), while for the high SARs (slots 4–7) the ~30% discrepancies observed are within the statistical errors (Fig. 3). The differences between theoretical and experimental SARs may be attributed to the high sensitivity of the thermo-optical sensor to even slight deviations from the tube's axial position and the non-linearity of the spatial distribution of the SAR.

Taking into account the applicability of the model for estimation of the SAR and the inability to measure it close to the tube walls, the SAR at the location of the cultures was calculated numerically. In Fig. 2C, the average SAR at the location of the cell cultures (0.2 mm from the bottom of the tubes) for tubes 4 and 6 is given. The local SAR at the position of the cells ranged between 2.75 ± 0.25 and 3.0 ± 0.25 W/kg in test tube 4 (mean 2.9 ± 0.2 W/kg) and between 3.65 ± 0.33 W/kg and 4.6 ± 0.6 W/kg (mean 4.1 ± 0.5 W/kg) in test tube 6. Thus cells placed in slot 4 were referred to as having been exposed to SAR of 2.9 W/kg and cells placed in slot 6 to 4.1 W/kg.

Effect of Temperature on Aneuploidy and Cell Proliferation

Exposure to increasing SARs is accompanied by a heating and a consequent increase in the temperature of the samples, which depends on the competition between the thermal input and dissipation to the surroundings. To avoid the possibility of heating the cells beyond the physiological range, we set the exposure incubator temperature at 33.5°C, which enabled us to compensate for the local heating in the sample during exposure, thereby maintaining the temperature of the exposed sample in the range of 36–37°C at the

TABLE 2
Incidence of Multisomy for Chromosomes 1, 10, 11 or 17 in Nuclei of Human Blood Lymphocytes Exposed *In Vitro* for 72 h to 800 MHz Radiation at SARs of 2.9 W/kg and 4.1 W/kg for each Individual Tested

	Control			2.9 W/kg			4.1W/kg		
Donor no.	No. scored	No. multisomic	Percentage multisomy	No. scored	No. multisomic	Percentage multisomy	No. scored	No. multisomic	Percentage multisomy
Chromosome 17									
1	1183	18	1.52	993	36	3.63	794	48	6.05
2	1100	53	4.82	848	33	3.89	1202	78	6.49
3	956	24	2.51	1000	86	8.60	1024	46	4.49
4	1365	41	3.00	1188	31	2.61	1138	47	4.13
5	1449	109	7.52	1006	111	11.03	1047	40	3.82
6	1262	45	3.57	722	56	7.76	1173	84	7.16
7	927	42	4.53	1330	75	5.64	1451	128	8.82
8	1762	194	11.01	1416	228	16.10	1418	163	11.50
9	992	102	10.28	1514	201	13.28	1346	210	15.60
10	1375	99	7.20	1185	159	13.42	1485	228	15.35
Chromosome 11									
1	1183	10	0.85	993	27	2.72	794	37	4.66
2	1100	20	1.82	848	18	2.12	1202	48	3.99
3	956	19	1.99	1000	35	3.50	1024	31	3.03
4	1365	21	1.54	1188	18	1.52	1138	34	2.99
5	1449	28	1.93	1006	60	5.96	1047	25	2.39
6	1262	25	1.98	722	35	4.85	1173	41	3.50
7	927	14	1.51	1330	44	3.31	1451	86	5.93
8	1762	95	5.39	1416	151	10.66	1418	87	6.14
9	992	60	6.05	1514	133	8.78	1346	137	10.18
10	1375	69	5.02	1185	124	10.46	1485	132	8.89
Chromosome 1									
6	953	57	5.98	1706	114	6.68	1641	128	7.80
7	1423	81	5.69	1218	65	5.34	1988	218	10.97
8	1555	136	8.75	674	92	13.65	1196	146	12.21
9	686	48	7.00	1234	168	13.61	1196	150	12.54
10	1471	87	5.91	1546	145	9.38	1543	139	9.01
Chromosome 10									
6	953	57	5.98	1706	84	4.92	1641	102	6.22
7	1423	64	4.50	1218	78	6.40	1988	262	13.18
8	1555	139	8.94	674	109	16.17	1196	160	13.38
9	686	24	3.50	1234	136	11.02	1196	118	9.87
10	1471	87	5.91	1546	147	9.51	1543	127	8.23

highest SAR used. Thus the sham samples in the exposure incubator were maintained at 33.5°C.

To test the effect of temperature on aneuploidy, we cultured PBLs obtained from four donors at different temperatures in the range of 33.5–40°C for 72 h. We examined the effect of temperature on the level of total aneuploidy (Fig. 4A and B) of chromosomes 11 and 17 as well as on the proliferative capacity of the cells (metaphase index; Fig. 4C). We found no statistically significant differences compared to cells at 37°C in spite of the slight decrease observed in aneuploidy as the temperature increased from 33.5 to 40°C. On the other hand, no significant difference was observed in the metaphase index at 38.5 and 40°C, while the level at 33.5°C was 35.6% of that at 37°C ($P = 0.03$).

In light of these results, we performed all comparisons of exposed samples with the controls grown at 37°C.

Effect of 72 h Exposure to 800 MHz RF Field on Aneuploidy

The basal levels of aneuploidy and gains of chromosomes 1, 10, 11 and 17 and the levels after exposure to two different SARs (2.9 W/kg and 4.1 W/kg) are given in Tables 1 and 2 for each individual tested. We observed a large variation in aneuploidy in unexposed PBLs derived from different donors. The aneuploidy after 72 h exposure of PBLs from an individual donor was higher in most cases than that in the corresponding unexposed culture. We observed a positive correlation between the basal aneuploidy level in the controls and the level in the corresponding exposed cultures for all the chromosomes studied and for each exposure level (Fig. 5). Thus the higher the basal aneuploidy level, the greater the level after RF-field exposure

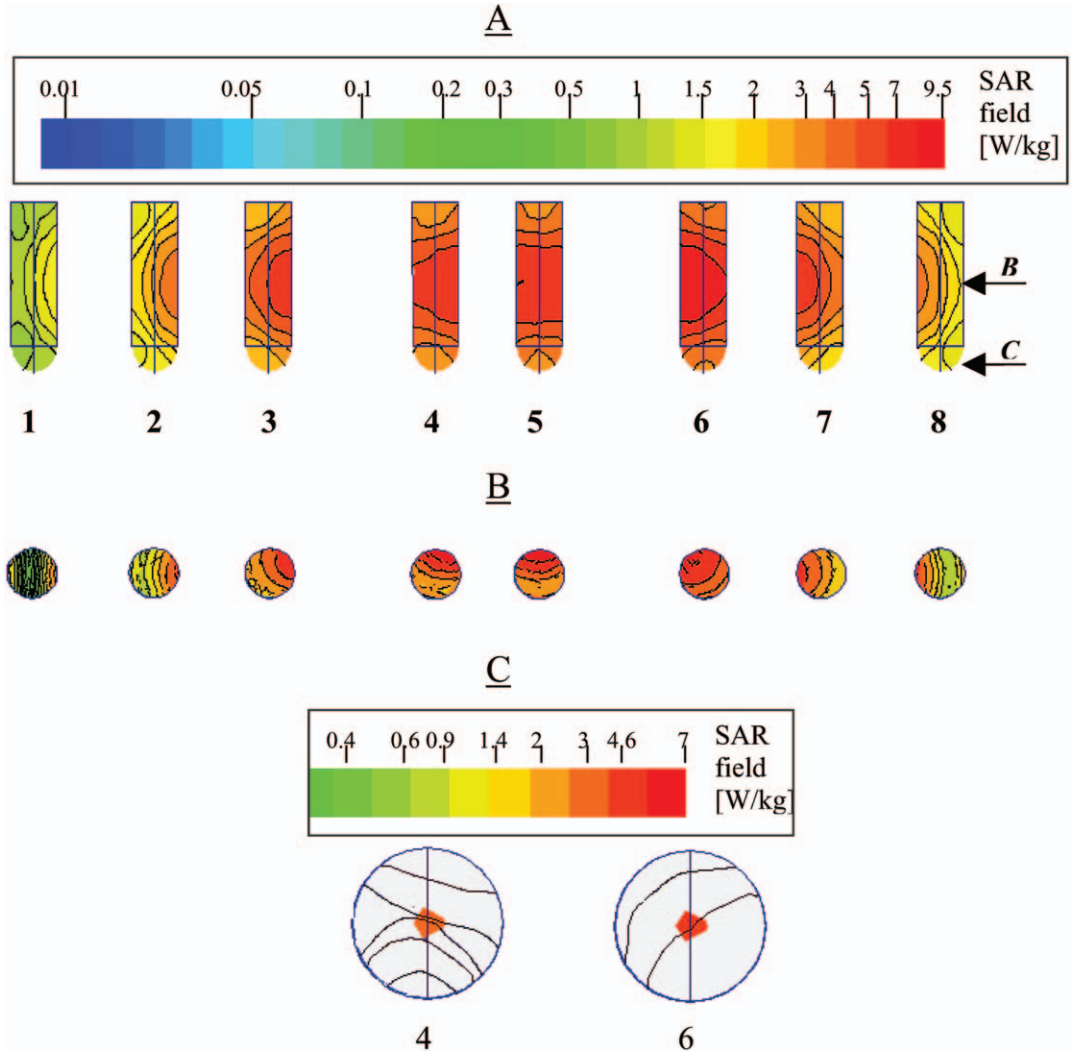

FIG. 2. Simulation of SAR distribution in exposure tubes. The simulation was performed using High Frequency Simulation Software (HFSS, Ansoft) for tubes filled with 5 ml of culture medium. Panel A: average SAR at the vertical median cross-section as a function of tube number (see Fig. 1). Panel B: Average SAR distribution at the horizontal median cross-section at the level shown by arrow B in panel A. The color scale for SAR is the same as in panel A. Panel C: Average SAR distribution on horizontal cross-section at cell location shown by arrow C in panel A.

(slope of 1.13 and 1.10 and R^2 of 0.58 and 0.60 for an SAR of 2.9 and 4.1 W/kg, respectively). This correlation was even more pronounced for chromosome gains, with a slope of 1.32 and 1.05 and R^2 of 0.71 and 0.57 for an SAR of 2.9 and 4.1 W/kg, respectively (data not shown). We observed a wide variation in aneuploidy between the donors for each of the chromosomes studied. This variation, defined as SD/mean $\times$ 100, was calculated to be 9.9% for chromosome 1, 7.7% for chromosome 10, 15.8% for chromosome 11, and 15% for chromosome 17. Therefore, we looked at the ratios of the exposed and control values to compensate for interindividual inhomogeneity.

The ratios of the aneuploidy of chromosomes 1, 10, 11 and 17 after the exposure to two different SARs (2.9 and 4.1 W/kg) and the appropriate controls are given in Fig. 6. The ratios of aneuploidy in exposed and control cultures were 1.23 $\pm$ 0.18 ($P = 0.044$) and 1.21 $\pm$ 0.22 ($P = 0.058$) at the higher SAR (4.1 W/kg) for chromosomes 1 and 10, respectively, while no statistically significant differences were observed at the lower SAR (2.9 W/kg). When we tested chromosomes 11 and 17, we found that the increase in aneuploidy was statistically significant at 2.9 W/kg ($P = 0.05$ and 0.04, respectively) but not at 4.1 W/kg.

These changes in the levels of aneuploidy are due to an increased proportion of cells harboring extra chromosomes (Fig. 7). For chromosome 1, the level of multisomy increased by 1.59 $\pm$ 0.26 ($P = 0.008$) after exposure to the higher SAR. In chromosome 10 there was no significant increase in the level of relative gains at either SAR. For chromosome 11, the level of multisomy increased by 2.03 $\pm$ 0.74 and 2.26 $\pm$ 1.38 in samples exposed at SARs of 2.9 W/kg and 4.1 W/kg, respectively, which was statisti-

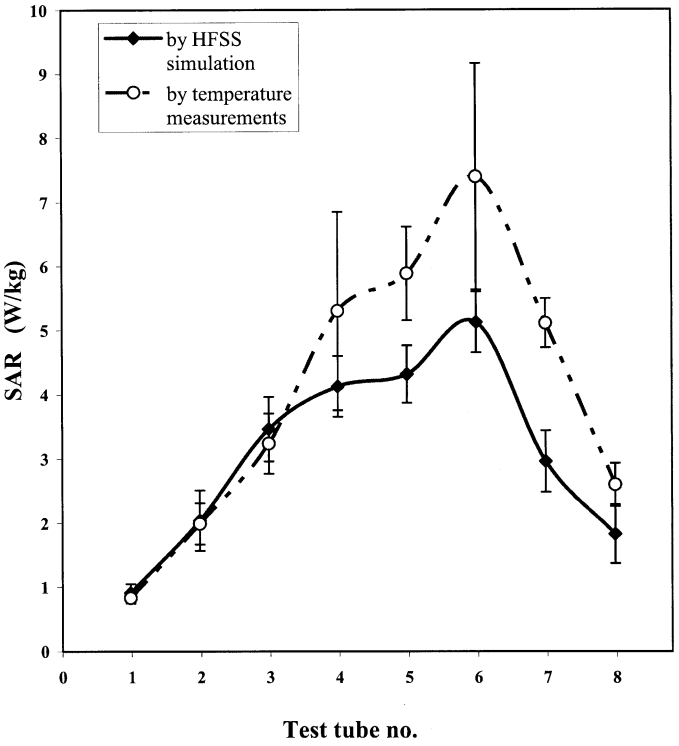

FIG. 3. Comparison of experimentally measured and simulated SARs. Test tubes were placed in positions 1–8 of the exposure system as in Fig. 1. The temperature in the test tubes was monitored using fiber-optic temperature sensors. The SARs were determined from the slope of the initial temperature increase in each tube during exposure. Data are means ± SD from at least five independent experiments. SARs were also computed from local SAR simulation by HFSS software with a 1-mm mesh for the locations of the temperature sensors as described in the Materials and Methods.

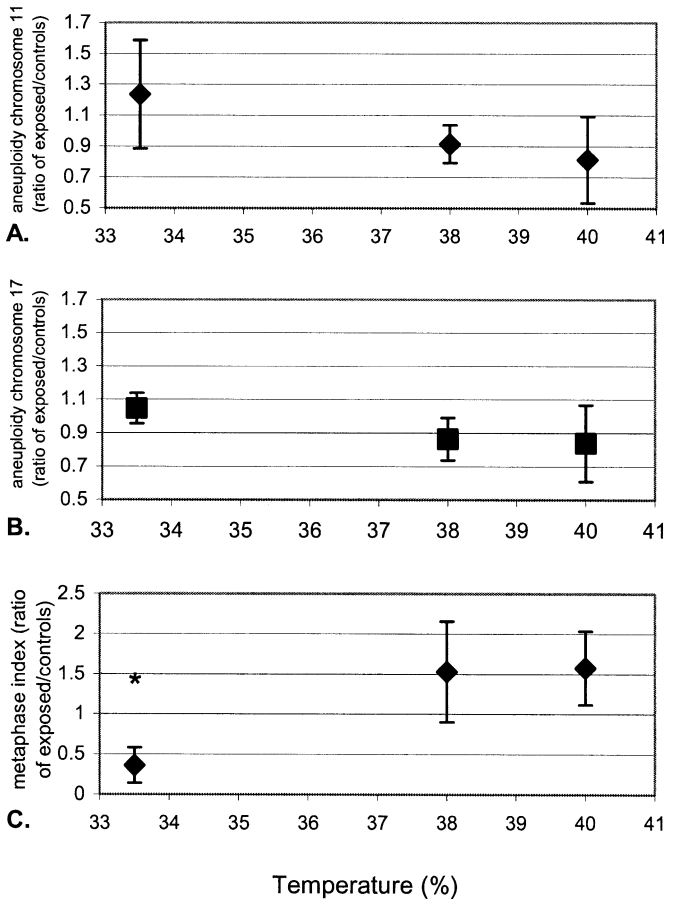

FIG. 4. Temperature dependence of aneuploidy of chromosomes 11 and 17 and of the metaphase index. The ratio of aneuploidy of chromosomes 11 (panel A) and 17 (panel B) in temperature-exposed and control lymphocytes. Panels C: The metaphase index ratio in temperature-exposed and control lymphocytes. Lymphocytes were incubated at 33.5, 38.5 and 40.0°C for 72 h and compared with those held at 37.0°C. Asterisk represents statistical significance at $P < 0.05$. $n = 4$.

cally significant compared to control levels ($P = 0.002$ and 0.017). For chromosome 17, the level of multisomy increased by 1.70 ± 0.79 and 1.76 ± 0.92 in samples exposed at SARs of 2.9 and 4.1 W/kg, respectively, which was statistically significant compared to control levels ($P = 0.021$ and 0.027).

DISCUSSION

To determine whether exposure to RF fields leads to an increase in genomic instability, a hallmark of cancer, we assayed the changes in aneuploidy in exposed cells. Aneuploidy was suspected to be a source of carcinogenesis by Boveri almost a century ago (*23*) and after an era devoted to the ''mutator phenotype'' as predisposing to cancer (*24*) has been regaining its central role (*3, 5, 7*). Aneuploidy arises due to failure of the mitotic apparatus and malsegregation of the chromosomes to the daughter cells whether due to failure in mitotic checkpoint, telomere shortening, or an increase in centrosome numbers (*25*). Others (*5, 11, 13, 26, 27*) have proposed that unbalanced nucleotide and metabolite pools due to the instigating insult cause and perpetuate the effect.

The determination of RF-field-induced aneuploidy in the published studies of other groups has been based on the micronucleus assay, which reflects the loss of DNA (either whole chromosomes or fragments). This approach is restricted to the determination of chromosomal loss (monosomy) and disregards the other constituent of aneuploidy, chromosomal gain (multisomy). In the present study, using interphase FISH, we determined the changes in both monosomy and multisomy. We examined aneuploidy in four chromosomes that harbor genes important in tumorigenesis: *HPC1* [chromosome 1 (28)], *PTEN* [chromosome 10 (*29*)], *ATM* [chromosome 11 (*30*)], and *TP53* [chromosome 17 (*10, 31–33*)].

The levels of aneuploidy that we observed in controls by semi-automatic image analysis of FISH images (16–22%) were similar to those reported in the literature using similar analytical approaches. van de Rijke *et al.* (*34*) reported that the level of aneuploidy of chromosome 7 in a normal diploid cell population was 30.8% and decreased to 8.7% after manual correction. Thus there is a discrepancy when com-

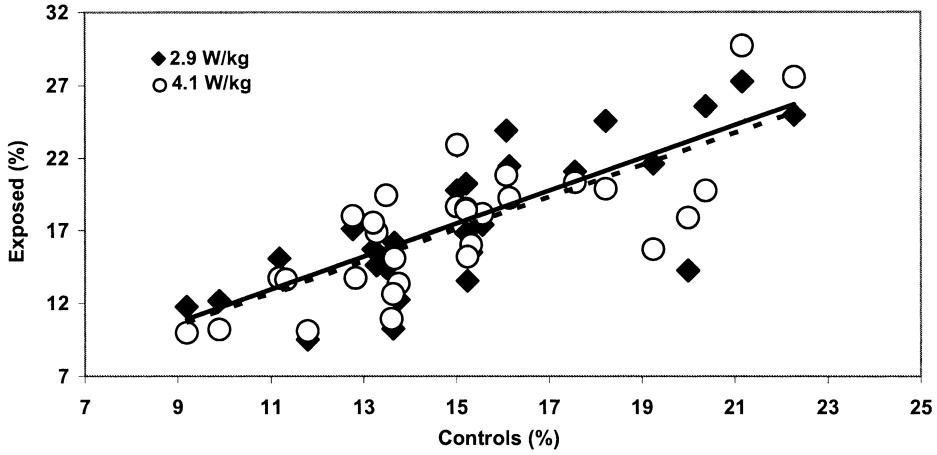

FIG. 5. Correlation of aneuploidy with and without exposure to 72 h of 800 MHz RF radiation. Solid diamonds and solid line, SAR of 2.9 W/kg; open circles and dotted line, SAR of 4.1 W/kg. The line for 2.9 W/kg is represented by the equation $y = 1.13x + 0.54$, with $R^2 = 0.58$. The line for 4.1 W/kg is represented by the equation $y = 1.10x + 0.54$, with $R^2 = 0.60$.

paring manual visual determination of the levels of aneuploidy by an experienced technician and automatic scoring based on image analysis of the three-dimensional nucleus. Most data in the literature come from metaphase and not interphase nuclei. We found no direct correlation between the aneuploidy levels at interphase and metaphase.[3] This is in agreement with the data of Zhang *et al.* (*35*), who found a marked difference in the levels of aneuploidy measured at metaphase and interphase and observed different trends for the effect of the chemical in the two parts of the cell cycle. These discrepancies are related to the limitations of the FISH assay as addressed by Eastmond *et al.* (*36*). One example is the overlapping signals resulting in excess monosomies.

The results presented here demonstrate that exposure to a CW RF field of 800 MHz for 72 h increased levels of aneuploidy at two SARs that depended on the chromosome studied as well as on the SAR. In chromosomes 1 and 10, there was a seemingly dose-dependent increase that was reversed for chromosomes 11 and 17 with increasing SAR. When looking at the levels of multisomy, which are the chief contributor to the increased aneuploidy, we observed a significant increase in chromosomes 1, 11 and 17 at the higher exposure level ($P \leq 0.05$), but the increase was not significant in chromosome 10 ($P = 0.058$). At the lower SAR, we saw no change in chromosome 1, leaving only chromosomes 11 and 17 affected. Thus, under our exposure conditions, we concluded that chromosomes 11 and 17 are the most vulnerable to the RF-field insult, chromosome 1 is the least vulnerable, and chromosome 10 is unaffected by the radiation. Similar chromosome sensitivity to low-intensity CW radiation at 100 GHz was recently observed by Korenstein-Ilan (unpublished results). The phenomenon of chromosome-specific aneuploidy has been demonstrated previously for different carcinogens (*37*) as well as during embryonic development (*38*). The origin of such chromosomal sensitivity is still unclear. It may be argued that inappropriate chromosomal segregation after exposure to RF radiation, leading to aneuploidy, is dependent on many different cellular components and is controlled by multiple signaling pathways, making the elucidation of the underlying mechanism extremely difficult.

The results presented here are in agreement with our previous findings of increased aneuploidy of chromosome 17 after 72 h *in vitro* exposure of human blood lymphocytes to a CW 835 MHz RF field at an average SAR of 1.6–8.8 W/kg (*21*). It should be pointed out that under the previous exposure conditions cells were exposed to a much more heterogeneous radiation than in the present study. When

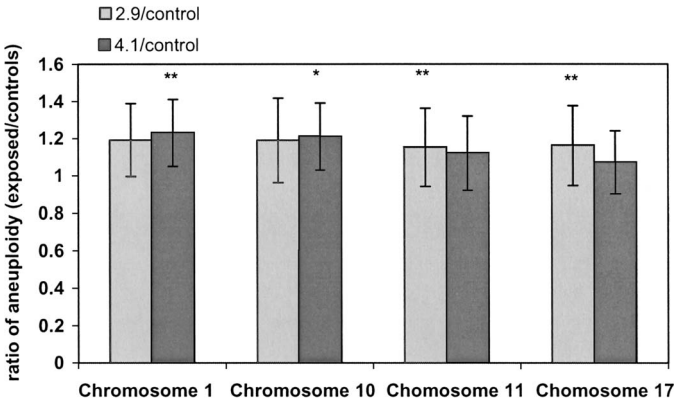

FIG. 6. Ratio of aneuploidy of chromosomes 1, 10, 11 and 17 in exposed and control lymphocytes after 72 h exposure to 800 MHz RF radiation at different SARs. The columns represent average ± SD of the aneuploidy in irradiated cells relative to controls. Gray columns, 2.9 W/kg; black columns, 4.1 W/kg; **statistically significant at $P < 0.05$; *$0.05 < P < 0.06$ compared to controls. For chromosomes 11 and 17, $n = 10$; for chromosomes 1 and 10, $n = 5$.

[3] P. Hasin, Aneuploidy in human peripheral blood lymphocytes following *in vitro* exposure to 0.1THz radiation. Dissertation, Tel-Aviv University, Tel-Aviv, Israel, 2005.

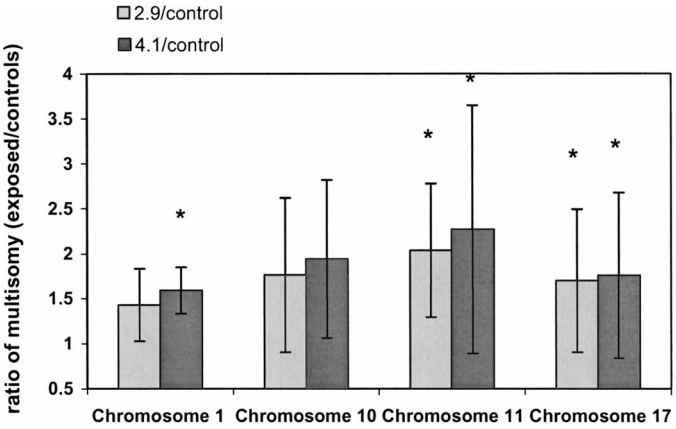

FIG. 7. Ratio of multisomy of chromosomes 1, 10, 11 and 17 in exposed and control lymphocytes after 72 h exposure to 800 MHz RF radiation at different SARs. The columns represent averages ± SD of the multisomy in irradiated cells relative to controls. Gray columns, 2.9 W/kg; black columns, 4.1 W/kg, ***statistically significant at $P < 0.01$; **statistically significant at $0.01 < P < 0.05$ and *$0.05 < P < 0.06$ compared to controls. For chromosomes 11 and 17, $n = 10$, for chromosomes 1 and 10 $n = 5$.

comparing the levels of aneuploidy for the average SARs in both experiments, we obtain comparable results. The previous study demonstrated 1.7- and twofold increases in aneuploidy of chromosome 17 for average SARs of 4.3 and 8.2 W/kg, respectively, while in the present study we observe 1.7 and 1.8 increase for average SAR of 2.9 W/kg and 4.1 W/kg, respectively. Furthermore, the lack of dependence of the level of aneuploidy of chromosome 17 on temperature in the range of 34.5–38.5°C was confirmed in the present study and was extended to chromosome 11. Most previous *in vitro* studies of the genetic consequences of exposure to RF radiation were restricted to periods of 24 h or less [for a recent review, see ref. (*2*)]. It has been shown that exposure of human PBLs to RF fields of 380, 900 and 1800 MHz for 48 or 68 h at SARs of 0.08, 0.2 and 1.7 W/kg, respectively, did not alter the frequencies of sister chromatid exchanges.

Separating ''thermal'' from ''athermal'' effects has long been controversial in evaluating the mechanisms underlying the effects of RF radiation on biological systems. This has been addressed previously using two different experimental conditions. One used exposure to radiation of a very low SAR that did not involve any substantial increase in the temperature of the exposed biological object. The other approach used radiation of an SAR that could elevate the temperature in the system but at the same time used environmental cooling to maintain a specified steady-state temperature SAR. We adopted the second approach by maintaining the exposed cells at a physiological temperature of 36–37°C at high SARs. The results of the control experiments in which cells were exposed to temperatures in the range of 33.5–40°C for 72 h demonstrate that aneuploidy is not sensitive to temperature changes in the range studied. However, one should bear in mind that the elevation of the sample's temperature by exposure to RF radiation differs from the elevation due to heat exchange with the external environment. Exposure to RF radiation leads to a direct heating of the sample, which then loses heat to the environment, while the conventional heating proceeds by heat conduction from the environment to the sample (*39, 40*). Naturally, the heating rates and exchanges are different under these different conditions, but they should lead to equal steady-state temperatures. It may be argued that convection patterns leading to fluid flow and to consequent circulation of cells may exist and may differ in the two situations. However, no indication of cell transport from the bottom of the exposed test tube into upper layers could be detected under either condition. These data suggest the possible existence of an athermal effect of RF radiation leading to increased levels of aneuploidy. These findings are in agreement with our previous study using a different type of exposure system (*21*) as well as other studies supporting the notion of athermal biological effects of RF radiation (*41–43*).

ICNIRP and IEEE, the two principal standard-setting organizations, used substantial safety factors in establishing limits for the exposure of workers and the general public, setting the average whole-body exposure limits for workers at 10 times lower than the accepted threshold for adverse effects. Limits for the general public were set to be 50 times lower than the threshold level to account for age, health and duration of exposure. The lowest SARs used in the present study are much higher than the ICNIRP threshold of 0.4 W/kg for average total-body exposure, but they are similar to the thresholds of 4 and 2 W/kg for localized exposure of the limbs and head-trunk, respectively (*44*). Thus the results of this study should be taken into consideration when assessing the health risk after continuous exposure to RF radiation at an SAR close to the current of thresholds set by ICNIRP.

ACKNOWLEDGMENTS

This work is based on a portion of a dissertations submitted by R. Mazor and Yael Eshet in partial fulfillment of the requirements for the M.Sc. degree to Tel-Aviv University. This research was funded by MAFAT/IMOD (coordinated by Dr. Abraham Sternlieb).

Received: November 1, 2006; accepted: September 4, 2007

REFERENCES

1. D. Brusick, R. Albertini, D. McRee, D. Peterson, G. Williams, P. Hanawalt and J. Preston, Genotoxicity of radiofrequency radiation. DNA/Genetox Expert Panel. *Environ. Mol. Mutagen.* **32**, 1–16 (1998).
2. Vijayalaxmi and G. Obe, Controversial cytogenetic observations in mammalian somatic cells exposed to radiofrequency radiation. *Radiat. Res.* **162**, 481–496 (2004).
3. R. Li, A. Sonik, R. Stindl, D. Rasnick and P. Duesberg, Aneuploidy vs. gene mutation hypothesis of cancer: recent study claims mutation but is found to support aneuploidy. *Proc. Natl. Acad. Sci. USA* **97**, 3236–3241 (2000).
4. P. Duesberg and R. Li, Multistep carcinogenesis: a chain reaction of aneuploidizations. *Cell Cycle* **2**, 202–210 (2003).

5. P. Duesberg and D. Rasnick, Aneuploidy, the somatic mutation that makes cancer a species of its own. *Cell Motil. Cytoskeleton* **47**, 81–107 (2000).
6. P. Dey, Aneuploidy and malignancy: an unsolved equation. *J. Clin. Pathol.* **57**, 1245–1249 (2004).
7. D. Grimm, Genetics. Disease backs cancer origin theory. *Science* **306**, 389 (2004).
8. D. Xu and R. L. Juliano, Epigenetic modulation of gene expression in mammalian cells. *Crit. Rev. Eukaryot. Gene Expr.* **15**, 93–101 (2005).
9. P. A. Jones, Overview of cancer epigenetics. *Semin. Hematol.* **42**, S3–S8 (2005).
10. A. Korenstein-Ilan, A. Amiel, S. Lalezari, M. Lishner and L. Avivi, Allele-specific replication associated with aneuploidy in blood cells of patients with hematologic malignancies. *Cancer Genet. Cytogenet.* **139**, 97–103 (2002).
11. P. Duesberg, A. Fabarius and R. Hehlmann, Aneuploidy, the primary cause of the multilateral genomic instability of neoplastic and preneoplastic cells. *IUBMB Life* **56**, 65–81 (2004).
12. S. Hanks, K. Coleman, S. Reid, A. Plaja, H. Firth, D. Fitzpatrick, A. Kidd, K. Mehes, R. Nash and Rahamn, Constitutional aneuploidy and cancer predisposition caused by biallelic mutations in BUB1B. *Nat. Genet.* **36**, 1159–1161 (2004).
13. P. Duesberg, Are centrosomes or aneuploidy the key to cancer? *Science* **284**, 2091–2092 (1999).
14. C. Lengauer and Z. Wang, From spindle checkpoint to cancer. *Nat. Genet.* **36**, 1144–1145 (2004).
15. A. Musio, D. Zambroni, P. Vezzoni and T. Mariani, Chromosomes, genes, and cancer breakpoints. *Cancer Genet. Cytogenet.* **139**, 141–142 (2002).
16. D. Pinkel, T. Straume and J. W. Gray, Cytogenetic analysis using quantitative, high-sensitivity, fluorescence hybridization. *Proc. Natl. Acad. Sci. USA* **83**, 2934–2938 (1986).
17. D. A. Eastmond and D. Pinkel, Detection of aneuploidy and aneuploidy-inducing agents in human lymphocytes using fluorescence *in situ* hybridization with chromosome-specific DNA probes. *Mutat. Res.* **234**, 303–318 (1990).
18. A. B. Mukherjee, V. V. Murty and R. S. Chaganti, Detection of cell-cycle stage by fluorescence *in situ* hybridization: its application in human interphase cytogenetics. *Cytogenet. Cell Genet.* **61**, 91–94 (1992).
19. T. Litmanovitch, M. M. Altaras, A. Dotan and L. Avivi, Asynchronous replication of homologous alpha-satellite DNA loci in man is associated with nondisjunction. *Cytogenet. Cell Genet.* **81**, 26–35 (1998).
20. A. Nagler, A. Korenstein-Ilan, A. Amiel and L. Avivi, Granulocyte colony-stimulating factor generates epigenetic and genetic alterations in lymphocytes of normal volunteer donors of stem cells. *Exp. Hematol.* **32**, 122–130 (2004).
21. M. Mashevich, D. Folkman, A. Kesar, A. Barbul, R. Korenstein, E. Jerby and L. Avivi, Exposure of human peripheral blood lymphocytes to electromagnetic fields associated with cellular phones leads to chromosomal instability. *Bioelectromagnetics* **24**, 82–90 (2003).
22. M. J. Barch, T. Knutsen and J. L. Spurbeck, Eds., *The AGT Cytogenetics Laboratory Manual.* Lippincott-Raven, Philadelphia, 1997.
23. T. Bovery, *Zur frage der Entsehung mailigner Tumoren.* Gustav Fischer Verlag, 1914.
24. L. A. Loeb, Mutator phenotype may be required for multistage carcinogenesis. *Cancer Res.* **51**, 3075–3079 (1991).
25. R. A. Bennett, H. Izumi and K. Fukasawa, Induction of centrosome amplification and chromosome instability in p53-null cells by transient exposure to subtoxic levels of S-phase-targeting anticancer drugs. *Oncogene* **23**, 6823–6829 (2004).
26. P. Duesberg, R. Li and D. Rasnick, Aneuploidy approaching a perfect score in predicting and preventing cancer: highlights from a conference held in Oakland, CA in January, 2004. *Cell Cycle* **3**, 823–828 (2004).
27. P. Duesberg, R. Stindl and R. Hehlmann, Explaining the high mutation rates of cancer cells to drug and multidrug resistance by chromosome reassortments that are catalyzed by aneuploidy. *Proc. Natl. Acad. Sci. USA* **97**, 14295–14300 (2000).
28. A. Rökman, T. Ikonen, E. H. Seppälä, N. Nupponen, V. Autio, N. Mononen, J. Bailey-Wilson, J. Trent, J. Carpten and J. Schleutker, Germline alterations of the RNASEL gene, a candidate HPC1 gene at 1q25, in patients and families with prostate cancer. *Am J. Hum. Genet.* **70**, 1299–1304 (2002).
29. L. Zhang, Q. Yu, J. He and X. Zha, Study of the PTEN gene expression and FAK phosphorylation in human hepatocarcinoma tissues and cell lines. *Mol. Cell. Biochem.* **262**, 25–33 (2004).
30. G. Rotman and Y. Shiloh, ATM: from gene to function. *Hum. Mol. Genet.* **7**, 1555–1563 (1998).
31. A. J. Levine, p53, the cellular gatekeeper for growth and division. *Cell* **88**, 323–331 (1997).
32. A. de la Chapelle and P. Peltomaki, The genetics of hereditary common cancers. *Curr. Opin. Genet. Dev.* **8**, 298–303 (1998).
33. D. H. Teng, R. Hu, H. Lin, T. Davis, D. Iliev, C. Frye, B. Swedlund, K. L. Hansen, V. L. Vinson and P. A. Steck, MMAC1/PTEN mutations in primary tumor specimens and tumor cell lines. *Cancer Res.* **57**, 5221–5225 (1997).
34. F. M. van de Rijke, H. Vrolijk, W. Sloos, H. J. Tanke and A. K. Raap, Sample preparation and *in situ* hybridization techniques for automated molecular cytogenetic analysis of white blood cells. *Cytometry* **24**, 151–157 (1996).
35. L. Zhang, N. Rothman, Y. Wang, R. B. Hayes, S. Yin, N. Titenko-Holland, M. Dosemeci, Y. Z. Wang, P. Kolachana and M. T. Smith, Benzene increases aneuploidy in the lymphocytes of exposed workers: a comparison of data obtained by fluorescence *in situ* hybridization in interphase and metaphase cells. *Environ. Mol. Mutagen.* **34**, 260–268 (1999).
36. D. A. Eastmond, M. Schuler and D. S. Rupa, Advantages and limitations of using fluorescence *in situ* hybridization for the detection of aneuploidy in interphase human cells. *Mutat. Res.* **348**, 153–162 (1995).
37. L. Zhang, W. Yang, A. E. Hubbard and M. T. Smith, Nonrandom aneuploidy of chromosomes 1, 5, 6, 7, 8, 9, 11, 12, and 21 induced by the benzene metabolites hydroquinone and benzenetriol. *Environ. Mol. Mutagen.* **45**, 388–396 (2005).
38. S. Munne, M. Bahce, M. Sandalinas, T. Escudero, C. Marquez, E. Velilla, P. Colls, M. Oter, M. Alikani and J. Cohen, Differences in chromosome susceptibility to aneuploidy and survival to first trimester. *Reprod. Biomed. Online* **8**, 81–90 (2004).
39. C. K. Chou and M. Swicord, Comment on ''Exposure of human peripheral blood lymphocytes to electromagnetic fields associated with cellular phones leads to chromosomal instability,'' by Mashevich et al. *Bioelectromagnetics* 2003;24(2):82–90. *Bioelectromagnetics* 24, 582 (2003).
40. A. Korenstein and R. Barbul, Reply to the comment on ''exposure of human peripheral blood lymphocytes to electromagnetic fields associated with cellular phones leads to chromosomal instability. *Bioelectromagnetics* **24**, 583–585 (2003).
41. E. Diem, C. Schwarz, F. Adlkofer, O. Jahn and H. Rudiger, Non-thermal DNA breakage by mobile-phone radiation (1800 MHz) in human fibroblasts and in transformed GFSH-R17 rat granulosa cells *in vitro*. *Mutat. Res.* **583**, 178–183 (2005).
42. S. Velizarov, P. Raskmark and S. Kwee, The effects of radiofrequency fields on cell proliferation are non-thermal. *Bioelectrochem. Bioenerg.* **48**, 177–180 (1999).
43. D. Leszczynski, S. Joenvaara, J. Reivinen and R. Kuokka, Non-thermal activation of the hsp27/p38MAPK stress pathway by mobile phone radiation in human endothelial cells: molecular mechanism for cancer- and blood–brain barrier-related effects. *Differentiation* **70**, 120–129 (2002).
44. Guidelines for limiting exposure to time-varying electric, magnetic, and electromagnetic fields (up to 300 GHz). International Commission on Non-Ionizing Radiation Protection. *Health Phys.* **74**, 494–522 (1998).